

NEAR-IR BRIGHT GALAXIES AT  $z \simeq 2$ . ENTERING THE SPHEROID FORMATION EPOCH ?<sup>1</sup>E. DADDI<sup>2</sup>, A. CIMATTI<sup>3</sup>, A. RENZINI<sup>2</sup>, J. VERNET<sup>3</sup>, C. CONSELICE<sup>4</sup>, L. POZZETTI<sup>5</sup>, M. MIGNOLI<sup>5</sup>, P. TOZZI<sup>6</sup>, T. BROADHURST<sup>7</sup>, S. DI SEREGO ALIGHIERI<sup>3</sup>, A. FONTANA<sup>8</sup>, M. NONINO<sup>6</sup>, P. ROSATI<sup>2</sup>, G. ZAMORANI<sup>5</sup>

Submitted 30 April 2003; Accepted 17 June 2003

## ABSTRACT

Spectroscopic redshifts have been measured for 9  $K$ -band luminous galaxies at  $1.7 < z < 2.3$ , selected with  $K_s < 20$  in the *K20 survey* region of the Great Observatories Origins Deep Survey area. Star formation rates (SFRs) of  $\sim 100\text{--}500 M_\odot \text{ yr}^{-1}$  are derived when dust extinction is taken into account. The fitting of their multi-color spectral energy distributions indicates stellar masses  $M \gtrsim 10^{11} M_\odot$  for most of the galaxies. Their rest-frame UV morphology is highly irregular, suggesting that merging-driven starbursts are going on in these galaxies. Morphologies tend to be more compact in the near-IR, a hint for the possible presence of older stellar populations. Such galaxies are strongly clustered, with 7 out of 9 belonging to redshift spikes, which indicates a correlation length  $r_0 \sim 9\text{--}17 h^{-1} \text{ Mpc}$  ( $1\sigma$  range). Current semianalytical models of galaxy formation appear to underpredict by a large factor ( $\gtrsim 30$ ) the number density of such a population of massive and powerful starburst galaxies at  $z \sim 2$ . The high masses and SFRs together with the strong clustering suggest that at  $z \sim 2$  we may have started to explore the major formation epoch of massive early-type galaxies.

*Subject headings:* galaxies: evolution — galaxies: formation — galaxies: high-redshift — galaxies: starbursts

## 1. INTRODUCTION

The remarkable success of the Cold Dark Matter (CDM) scenario to account for the cosmic microwave background power spectrum (Bennett et al. 2003), leaves understanding galaxy formation and evolution as one of the most compelling, unresolved issues of present cosmology. Semianalytical renditions of CDM hierarchical paradigm have so far favored a slow growth with time, with a major fraction of the mass assembly taking place at  $z \lesssim 1$  (e.g., Baugh et al. 2002; Somerville, Primack, & Faber 2001), with virtually all massive galaxies disappearing by  $z \sim 1.5$ . Recent results from the K20 project (Cimatti et al. 2002a,b,c; Daddi et al. 2002; Pozzetti et al. 2003) appear to be at variance with these expectations. The K20 project consists of a spectroscopic survey of  $\sim 500 K_s < 20$  objects selected over 52 arcmin<sup>2</sup>, and has revealed a sizable high redshift tail in the galaxy redshift distribution, where  $\sim 30$  galaxies ( $\sim 6\%$  of the total sample) were found at  $z > 1.7$ . Semianalytical CDM models would have predicted no galaxy at all at such high redshifts in the whole sample (see Fig. 4 in Cimatti et al. 2002c). The redshift distribution could be reproduced with pure luminosity evolution (PLE) models, although not for all realizations (see also Somerville et al. 2003). However, for only a few among the  $z \gtrsim 1.5$  galaxies was a spectroscopic redshift available, while for all other such galaxies only the photometric redshifts could be obtained. In order to put on firmer grounds such major result of the K20 project (and to understand the nature of these high- $z$  galaxies) we have conducted new VLT spectroscopic observations of galaxies with either photometric or

(uncertain) spectroscopic redshift above  $z \sim 1.7$ . This letter reports the results of the new spectroscopic observations, and combines them with the optical HST+ACS and infrared VLT+ISAAC imaging made available by the Great Observatories Origins Deep Survey (GOODS) project (Giavalisco et al. 2003). We assume a Salpeter IMF;  $\Omega_\Lambda, \Omega_M = 0.7, 0.3$ , and  $h = H_0 [\text{km s}^{-1} \text{ Mpc}^{-1}] / 100 = 0.7$ .

## 2. THE SPECTROSCOPIC SAMPLE

A sample of 20 galaxies with photometric redshifts  $z_{\text{phot}} \gtrsim 1.7$  were selected among the 41 galaxies without spectroscopic redshift identification in the 32 arcmin<sup>2</sup> K20 field that is included in the GOODS-South area. The photometric redshifts were improved over an earlier estimate (Cimatti et al. 2002b) by including the ultra-deep *JHKs* photometry from the GOODS VLT+ISAAC imaging. Within this sample, 10 objects with most secure  $z_{\text{phot}}$  have been observed in November 2002 with VLT+FORS2, integrating for 7.2ks with 0''.6 seeing, and using the 300V grism covering the range 3600–8000 Å with 13 Å resolution for a 1'' slit.

The spectra were reduced and calibrated in a standard way (Cimatti et al. 2003b) and co-added to already existing spectra, when available. Redshifts were measured for 7 galaxies from absorption features in their blue continua identified as UV metal lines (Fig. 1). For the  $z > 2$  galaxies Ly $\alpha$  in absorption and the onset of Ly $\alpha$  forest are also detected. One galaxy (ID#5) shows HeII $\lambda 1640$  and CIII] $\lambda 1909$  emission lines. Hints for those emission lines are found also for object ID#9, for which redshift is less secure because of the faint and noisy spectrum. Together with 2 previously identified galaxies (ID#1 and ID#2), a sample of 9 galaxies with spectroscopic redshift  $z_{\text{spec}} > 1.7$  is now available among the 304  $K_s < 20$  galaxies in the K20/GOODS-South area (Table 1). Correspondingly, the fraction of  $K_s < 20$  galaxies with  $z_{\text{spec}} > 1.7$  is  $3.0^{+2.8\%}_{-1.4\%}$ , for a surface density of  $0.28^{+0.26}_{-0.13} \text{ arcmin}^{-2}$ , and a comoving density of  $4.6^{+4.3}_{-2.2} \times 10^{-4} h^3 \text{ Mpc}^{-3}$  (the range  $1.7 < z < 2.25$  is used, hereinafter, for volume calculations). The uncertainties are poissonian at the 95% c.l. Accounting for cosmic variance due to clustering (Sect.

<sup>1</sup> Based on observations collected at the European Southern Observatory, Chile (ESO programs 70.A-0140, 168.A-0485), and with the NASA/ESA *Hubble Space Telescope*, obtained at the Space Telescope Science Institute, which is operated by AURA Inc. under NASA contract NAS 5-26555.

<sup>2</sup> ESO, Karl-Schwarzschild-Str. 2, D-85748 Garching, Germany

<sup>3</sup> Osservatorio Astrofisico di Arcetri, L.go E. Fermi 5, Firenze, Italy

<sup>4</sup> Caltech, Mail code 105-24, Pasadena (CA) 91125

<sup>5</sup> Osservatorio Astronomico di Bologna, via Ranzani 1, Bologna, Italy

<sup>6</sup> Osservatorio Astronomico di Trieste, via Tiepolo 11, Trieste, Italy

<sup>7</sup> Racah Institute for Physics, The Hebrew University, Jerusalem, Israel

<sup>8</sup> Oss. Astron. di Roma, via Dell'Osservatorio 2, Monteporzio, Italy

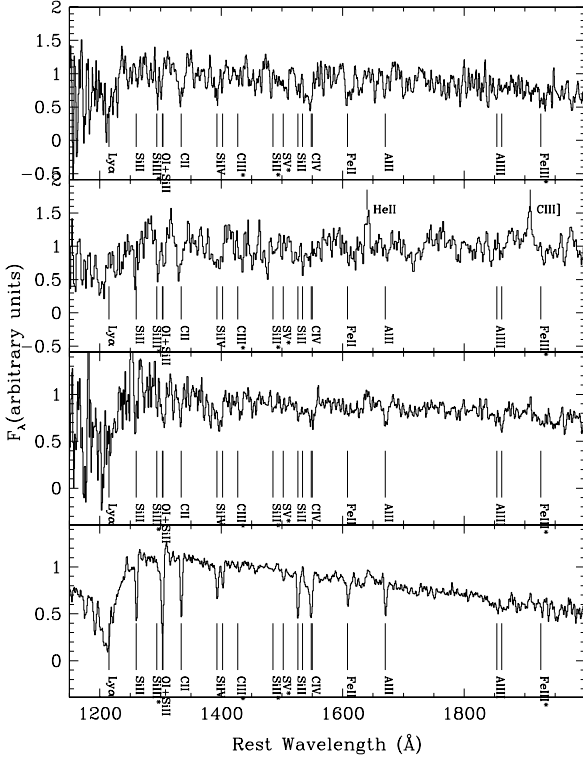


FIG. 1.— The panels show the spectra of, from top to bottom: (1) ID#7 at  $z = 2.227$ ; (2) ID#5, the X-ray and radio source at  $z = 2.223$ ; (3) the average spectrum of  $8 z > 1.7$  K-band luminous galaxies (ID#2 has only a near-IR spectrum showing  $H\alpha$  emission) (4) the average spectrum of  $\sim 250$  LBGs with  $\text{Ly}\alpha$  in absorption (Shapley et al. 2003). The principal metal lines observed in the UV for starburst galaxies are marked for reference, namely the ISM lines  $\text{SiII}\lambda 1260, 1304, 1527, 1534$ ;  $\text{OII}\lambda 1303$ ,  $\text{CII}\lambda 1334.5$ ,  $\text{CIV}\lambda 1548, 1551$ ,  $\text{SiIV}\lambda 1394, 1403$ ,  $\text{FeII}\lambda 1608$ ,  $\text{AlIII}\lambda 1671$ ,  $\text{AlIII}\lambda 1855, 1863$ ; as well as the photospheric absorption lines (shown with an asterisk)  $\text{FeIII}\lambda 1926$ ,  $\text{SV}\lambda 1502$ ,  $\text{SiIII}\lambda 1294$ ,  $\text{SiII}\lambda 1485$ ,  $\text{CIII}\lambda 1427$ .

3) would significantly alter only the upper bounds (see e.g. Eq. 8 in Daddi et al. 2000). These densities would increase by a factor of two by including the remaining objects with  $z_{\text{phot}} \gtrsim 1.7$ . The good agreement between  $z_{\text{phot}}$  and  $z_{\text{spec}}$  in the poorly tested region  $1.7 < z < 2.3$  (Table 1) suggests a fair fraction of the latter to be genuine  $z \sim 2$  galaxies. Obtaining  $z_{\text{spec}}$  for these is difficult due to their redder colors and thus fainter optical magnitudes with respect to galaxies with measured  $z_{\text{spec}}$ .

### 3. PROPERTIES OF K-BAND LUMINOUS GALAXIES AT $z \sim 2$

Using the wealth of subsidiary data available on the GOODS-South area we investigate in this section the nature of these  $K$ -band luminous galaxies with  $z_{\text{spec}} \sim 2$ .

— *Star formation rates.* The rest-frame UV spectra of these galaxies indicate that they are actively star-forming. They are very similar to the template Lyman Break Galaxies (LBG) spectrum (Shapley et al. 2003), and often show  $\text{SiIII}\lambda 1294$  absorption due to OB stars (Fig. 1).  $\text{Ly}\alpha$  emission is never detected, as for 25–50% of LBGs (Shapley et al 2003), a hint for significant dust extinction. The UV fluxes at  $2800\text{\AA}$  correspond to star formation rates ( $SFRs$ ) in the range of  $\sim 10$ – $40$   $\text{M}_\odot \text{yr}^{-1}$  before extinction correction (Kennicutt 1998). The extinction at  $1600\text{\AA}$  was estimated from the UV spectral slope  $\beta$  (Meurer et al. 1999) derived from the multicolor photometry. The  $SFRs$  derived in this way (adopting the Calzetti

et al. 2000 extinction law) are very high, with a median of  $\approx 400 \text{ M}_\odot \text{yr}^{-1}$ . As an alternative estimate *hyperz* was used (Bolzonella et al. 2000) to fit Bruzual & Charlot model spectral energy distributions (SED) to the observed ones from the available deep VLT BVRIZJHKs photometry, assuming constant  $SFR$  (CSF), and solar metallicity. The best fitting models require reddening in the range  $E(B-V) \sim 0.3$ – $0.6$  and intense  $SFRs$  up to  $\sim 500 \text{ M}_\odot \text{yr}^{-1}$ , with a median of  $150 \text{ M}_\odot \text{yr}^{-1}$ . Using a SMC extinction law would lower both the  $SFRs$  and  $E(B-V)$  estimates. Interestingly, ID#5 (which has the highest extinction-corrected  $SFR$ ) is a faint (soft) X-ray source (XID563 in the Chandra Deep Field South catalog, Giacconi et al. 2002). If completely due to star formation, its X-ray luminosity  $L_{2-10\text{keV}} \sim 2.7 \times 10^{42} \text{ erg s}^{-1} \text{ cm}^{-2}$  corresponds to  $SFR \approx 500 \text{ M}_\odot \text{yr}^{-1}$  (Nandra et al. 2002). The object is also a faint 1.4 Ghz radio source with a flux density of  $103 \pm 13 \mu\text{Jy}$  (Kellermann et al. 2003, private communication), fully consistent with the tight X-ray–radio luminosities correlation shown by Ranalli et al. (2003) for actively star-forming galaxies. We cannot definitively rule out the presence of an obscured AGN, but the lack of AGN signatures in its UV spectrum, showing instead a strong  $\text{SiIII}\lambda 1294$  photospheric absorption line, the non detection in the Chandra hard band and the low X-ray to optical flux ratio ( $\log(f_{0.5-2\text{kev}}/f_R) \sim -1.3$ ) indicate this is a vigorous star-forming galaxy. The stacked X-ray fluxes of the undetected sources give a  $2\sigma$  detection corresponding to  $< SFR > \approx 100 \text{ M}_\odot \text{yr}^{-1}$  ( $\Gamma = 2.1$  is assumed following Brusa et al. 2002). In general the limits on the X-ray luminosities ( $L_X \lesssim 10^{42} \text{ erg s}^{-1} \text{ cm}^{-2}$ ) and the low X-ray to optical flux ratios ( $\log(f_{0.5-2\text{kev}}/f_R) \lesssim -1.5$ ) imply that our sample contains virtually no AGN. The high  $SFRs$  qualify these galaxies as *starbursts*, and allow to build up the equivalent of a local  $M^* \sim 10^{11} \text{ M}_\odot$  galaxy in 0.2–1 Gyr.

— *Stellar masses.* Although the SEDs are reddened in the rest-frame UV, they appear even redder toward the near-IR, where they show a steep flux increase, starting in the F850LP band or beyond, which is suggestive of relatively old stellar populations. The CSF models discussed above imply  $M_{\text{stars}} = 0.3 - 5.5 \times 10^{11} \text{ M}_\odot$ , and luminosity-weighted ages of about 250–1700 Myr. In this case, the near-IR bump is reproduced by a prominent Balmer break. The CSF models are likely to underestimate the masses of the galaxies, as older stars, with higher mass to light ratios, may well be present and yet their light would be outshined by the younger ones. In order to estimate reliable upper limits, the minimal contribution to the  $K$ -band light by the ongoing starburst is determined by fitting a very young ( $\lesssim 10$  Myr) reddened component to the SEDs between the  $B$  and  $I$  bands. This component accounts for 30–50% of the  $K$ -band light. Assuming the remaining  $K$ -band light is due to a maximally old 3 Gyr stellar-population component, the resulting masses are typically a factor of 2–5 higher than estimated from CSF models, similarly to what is found for LBGs (Papovich et al. 2001).

— *Clustering.* Significant redshift pairing is observed among  $z \sim 2$  galaxies, a clear indication of strong clustering. Monte Carlo simulations are used to constrain the correlation length  $r_0$  from the short scale pairing, assuming a slope  $\gamma = 1.8$  for the correlation function (Daddi et al. 2002). A flat selection function between  $z = 1.7$  and  $z = 2.25$  is used. Seven independent pairs within  $5 \text{ h}^{-1}$  comoving Mpc are found in our sample of 9 galaxies, implying  $r_0 > 7 \text{ h}^{-1}$  Mpc comoving (95% c.l.), and a most likely range  $9$ – $17 \text{ h}^{-1}$  Mpc (68% c.l.).

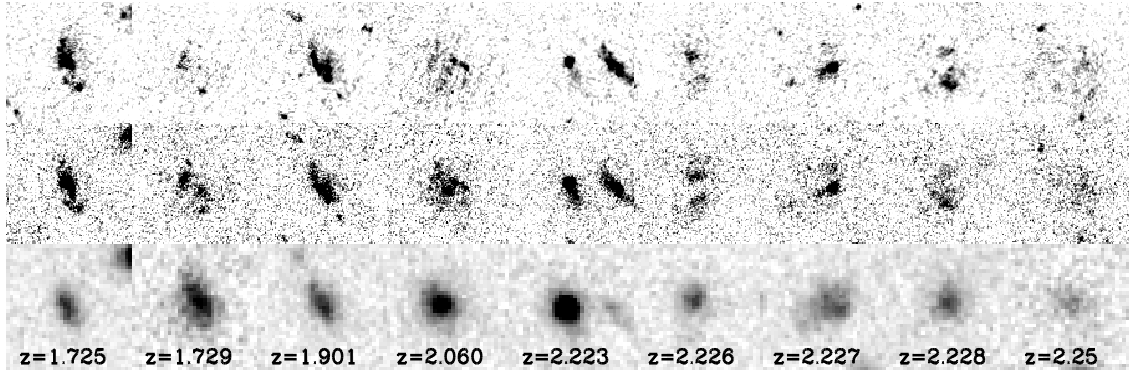


FIG. 2.— ACS (top and center row for F435W and F850LP respectively, epochs 1+2+3) and VLT+ISAAC (bottom row for  $K_s$ , seeing  $0.5''$ ) imaging for the galaxies with spectroscopic identification. The images are  $5''$  on a side. Redshift measurement for each galaxy is given in the bottom panels.

TABLE 1.  $K$ -BAND LUMINOUS STARBURSTS AT  $z > 1.7$  IN THE K20/GOODS AREA

| ID  | $z_{\text{spec}}$ | $z_{\text{phot}}$ | $K_s$<br>Vega | $J-K_s$<br>Vega | $R-K_s$<br>Vega | $\beta$ | $SFR_{\text{UV}}$<br>$M_{\odot}/\text{yr}$ | $SFR$<br>$M_{\odot}/\text{yr}$ | $E(B-V)$ | $t$<br>Gyr | $M$<br>$10^{10} M_{\odot}$ | $r_{\text{hl}}$<br>'' | $r_{\text{hl}}$<br>kpc | C   | A    | S   |
|-----|-------------------|-------------------|---------------|-----------------|-----------------|---------|--|--------------------------------|----------|------------|----------------------------|-----------------------|------------------------|-----|------|-----|
| (1) |                   |                   |               |                 |                 | (2)     | (3)  | (4)                            | (4)      | (4)        | (4)                        | (5)                   | (5)                    | (5) | (5)  | (5) |
| 1   | 1.727             | 1.74              | 19.99         | 1.44            | 3.15            | -0.7    | 26   | 93                             | 0.3      | 0.36       | 3.4                        | 0.6                   | 4.8                    | 2.2 | 0.21 | 0.9 |
| 2   | 1.729             | 2.54              | 19.07         | 1.99            | 4.54            | 0.7     | 13   | 490                            | 0.6      | 0.25       | 11                         | 0.8                   | 7.1                    | 1.8 | 0.30 | 1.4 |
| 3   | 1.901             | 1.65              | 19.68         | 1.57            | 3.42            | -0.9    | 27   | 155                            | 0.3      | 0.52       | 7.9                        | 0.6                   | 5.4                    | 1.9 | 0.41 | 0.6 |
| 4   | 2.060             | 1.78              | 19.31         | 1.83            | 4.15            | -0.2    | 35   | 487                            | 0.5      | 0.50       | 25                         | 0.7                   | 5.9                    | 2.0 | 0.34 | 1.3 |
| 5   | 2.223             | 2.40              | 18.72         | 2.15            | 4.15            | 0.0     | 38   | 540                            | 0.4      | 1.0        | 55                         | 0.4                   | 3.5                    | 3.2 | 0.25 | 0.3 |
| 6   | 2.226             | 2.24              | 19.94         | 1.69            | 3.30            | -0.4    | 18   | 88                             | 0.3      | 0.71       | 6.0                        | 0.7                   | 5.5                    | 2.6 | 0.33 | 0.5 |
| 7   | 2.227             | 2.11              | 19.45         | 1.80            | 3.46            | -1.2    | 31   | 178                            | 0.3      | 0.72       | 13                         | 0.7                   | 5.5                    | 2.2 | 0.41 | 1.3 |
| 8   | 2.228             | 2.43              | 19.74         | 2.02            | 3.66            | -0.4    | 26   | 121                            | 0.3      | 1.4        | 17                         | 0.9                   | 7.8                    | 2.1 | 0.25 | 0.9 |
| 9   | 2.25              | 2.29              | 19.94         | 1.94            | 3.65            | -0.7    | 30   | 153                            | 0.3      | 1.7        | 26                         | 1.1                   | 9.4                    | 2.7 | 0.29 | 1.2 |

NOTE. — (1) The redshift for ID#9 is less secure. (2) UV spectral slope. Typical errors are  $\pm 0.1$ . (3)  $SFR$  derived from the  $2800\text{\AA}$  luminosity without extinction correction. (4) Star formation rate, extinction, luminosity weighted stellar age and stellar mass derived from SED fitting of CSF models with reddening. (5) Quantities measured in the F850LP band, typical errors are  $\Delta C, \Delta A, \Delta S = 0.15, 0.15, 0.05$ .

— *Morphology.* In the HST+ACS and VLT+ISAAC images taken for the GOODS project all galaxies show a rather irregular light distribution (Fig. 2), with bright knots and low surface brightness regions, often split into separated components. We measured the *CAS* parameters (Conselice 2003; Bershady et al. 2000; and references therein), finding relatively high clumpiness ( $S$ ), high asymmetry ( $A$ ) and very low concentration ( $C$ ) (see Table 1). As  $S$  is known to correlate with the  $SFR$ s, the large  $S$  values are consistent with the high  $SFR$ s estimated above. The  $A$  values of most galaxies are consistent within the errors with the limit of  $A > 0.35$ , typical of galaxies undergoing merging or that experienced merging in the last Gyr (Conselice 2003). The low  $C$  values are also typical of local merging-driven starbursts, or ultra luminous infrared galaxies (ULIRGs). There is a trend for increasing  $C$  from the rest frame far-UV (F435W band) to the optical ( $K$ -band, resolution effects having been taken into account), implying a morphological  $K$ -correction. Also this is typical of starburst galaxies (see e.g. Dey et al. 1999; Smail et al. 2003), and may indicate the presence of an older bulge/disk component (e.g. Labb   et al. 2003b) or a higher reddening in the central regions. All the galaxies appear rather extended, allowing to host the high estimated  $SFR$ s. The average half light radius is  $r_{\text{hl}} = 0''.7$  in the F850LP band, about  $\sim 6$  kpc.

#### 4. RELATING TO OTHER $z \gtrsim 2$ GALAXY POPULATIONS

We now compare the properties of these  $K$ -band luminous galaxies to those of other relevant populations at  $z \gtrsim 2$ , namely: LBGs at  $z \sim 3$ , very red  $z > 2$  galaxies, and SCUBA

sources. Compared to LBGs (e.g. Giavalisco et al. 2002), these near-IR bright starbursts at  $z \sim 2$  have, on average, larger sizes, higher masses and  $SFR$ s, and stronger clustering. Despite their spectral similarity, these galaxies are not just a special subsample of LBGs. Indeed, it appears that they have redder UV continuum than the reddest LBGs template (Fig. 1). In fact, most objects in Table 1 have  $\beta > -1$ , while most LBGs have UV slopes between  $\beta = -2$  to  $-1$ , and virtually none has  $\beta > -0.5$  (Adelberger & Steidel 2000). Hence, the two populations appear only partially overlapping.

These  $z \sim 2$  starbursts are red in the near-IR, with  $J-K \gtrsim 1.7$ , and their clustering is consistent with that of much fainter  $K_s < 24$  galaxies at  $z > 2$  with  $J-K > 1.7$  colors (Daddi et al. 2003). In fact, van Dokkum et al. (2003) found significant redshift pairing among 5 galaxies at  $z > 2$  selected with  $J-K > 2.3$  (Franx et al. 2003; Labb   et al. 2003a). Nevertheless, the two samples show different properties, as strong  $Ly\alpha$  emissions, regular morphologies, and AGN signatures are common among van Dokkum et al. objects. Our 9 spectroscopically confirmed galaxies have  $J-K < 2.3$  and very clumpy and asymmetric morphologies. We conclude that there is a large variety of properties among  $K$ -band bright galaxies at  $z > 2$ , that we are just starting to explore.

Given the estimated  $SFR$ s, redshift range and peculiar morphology, some of our galaxies are potential SCUBA sources (Chapman 2003a,b). Red UV SEDs with  $\beta > -0.5$  are indeed common among SCUBA sources (e.g. Dey et al. 1999, Chapman et al. 2002), which also appear to have large clustering (e.g. Webb et al. 2003). Nevertheless, SCUBA sources

have much lower spatial density and are often much fainter than  $K_s = 20$ , while some of our sources may have too low *SFRs* to be submm-bright. Hence, also in this case the two populations are likely to overlap only partially.

## 5. DISCUSSION

These *K*-band luminous starbursts provide a substantial contribution to the cosmic *SFR* density (*SFRD*) at  $z \sim 2$ : adding up the *SFRs* from SED modeling we derive *SFRD*  $\sim 0.04 \text{ M}_\odot \text{ yr}^{-1} \text{ Mpc}^{-3}$  from the 9 spectroscopically confirmed galaxies alone. This estimate is certainly affected by incompleteness, and yet it already represents  $\sim 30\text{--}60\%$  of the *SFRD* within the range  $1.5 < z < 3$  (see e.g. the compilation by Nandra et al. 2002). These galaxies are also among the most massive systems detected at  $z \sim 2$ . Six objects in our sample have  $M_{\text{stars}} > 10^{11} \text{ M}_\odot$  (conservative estimates), resulting in a number density  $\sim 10^{-4} \text{ Mpc}^{-3}$  and a mass density of  $\sim 2 \times 10^7 \text{ M}_\odot \text{ Mpc}^{-3}$ , both  $\approx 10\%$  of the corresponding local value (Cole et al. 2001). Integrating over the mass function predicted by the Baugh et al. (2002) model at  $z = 1.92$ , one expects on average only 0.2 galaxies with  $M_{\text{stars}} > 10^{11} \text{ M}_\odot$  within the explored volume, and even less if the semianalytical mass function was properly normalized at  $z = 0$ . Therefore, these semianalytical models underestimate the number of massive galaxies at  $z \sim 2$  by about a factor of 30, and possibly much more given the incompletenesses of our spectroscopic sample. The assembly of massive galaxies apparently took place at a significantly larger redshift (earlier epoch) than predicted by the models (see also Genzel et al. 2003). On the other hand, these  $z \sim 2$  galaxies are too actively star-forming and irregular to be consistent with PLE models with high redshift of formation. The agreement between the observed redshift distribution at  $z > 1.7$  and the PLE model described in Cimatti et al. (2002c) is therefore likely to be just chance.

These *K*-band luminous starbursts are very strongly clustered, suggesting they are hosted in very massive and biased environments, which itself argues for these objects

being quite massive. At  $z < 2$  the only known sources with  $r_0 \gtrsim 7 \text{ h}^{-1} \text{ Mpc}$  are old, passively evolving EROs (Daddi et al. 2000, 2001) and local massive ellipticals (Norberg et al. 2002). These  $z \sim 2$  galaxies are therefore likely to evolve into such classes of objects. If star-formation ends rapidly, it would take them  $\gtrsim 1 \text{ Gyr}$  to develop very red optical to near-IR colors and to morphologically relax to regular bulge-dominated galaxies. This scenario, with massive spheroids still forming at  $z \sim 2\text{--}3$ , would be quite in good agreement with some properties of  $z \sim 1$  old EROs, including their number counts (Daddi, Cimatti & Renzini 2000), hints for residual star-formation present in their UV rest-frame (McCarthy et al. 2001), and with the inferred formation redshifts ( $2.4 \pm 0.3$ ) of their stellar populations (Cimatti et al. 2002a). At the same time, it would predict a paucity of passive EROs at, say,  $z > 1.3\text{--}1.5$ . Finally, we notice that a major shift seems to happen for the clustering properties of star-forming galaxies from  $z \sim 1$ , where they have very low clustering (see e.g. Daddi et al. 2002), to  $z \sim 2$ , where they have a very large one. The straightforward interpretation is that while at  $z \lesssim 1$  star formation is mostly confined to low-mass galaxies, at  $z \sim 2$  we are starting to see the major build up phase of massive early-type galaxies. It remains to be determined whether this  $z \sim 2$  activity represents the peak or the low- $z$  tail of the massive spheroid formation epoch. With the existing technology we should soon be able to answer this question, mapping massive galaxy assembly as a function of both redshift and large scale structure environment.

## REFERENCES

- Adelberger K. L., Steidel C. C., 2000, ApJ, 544, 218  
 Baugh C.M., Benson A.J., Cole S., et al., 2002, in ‘The Mass of Galaxies at Low and High Redshift’, eds. R. Bender, A. Renzini (astro-ph/0203051)  
 Bennett C.L., et al., 2003, submitted to ApJ (astro-ph/0302207)  
 Bershady M.A., Jangren J.A., Conselice C.J. 2000, AJ, 119, 2645  
 Brusa M., Comastri A., Daddi E., et al., 2002, ApJ, 581, L89  
 Bolzonella M., Miralles J.-M., Pelló R., 2000, A&A, 363, 476  
 Calzetti D., Armus L., Bohlin R. C., et al., 2000, ApJ, 533, 682  
 Cimatti A., Daddi E., Mignoli M., et al., 2002a, A&A 381, L68  
 Cimatti A., Mignoli M., Daddi E., et al., 2002b, A&A 392, 395  
 Cimatti A., Pozzetti L., Mignoli M., et al., 2002c, A&A 391, L1  
 Chapman S. C., Shapley A., Steidel C., Windhorst R., 2002, ApJ, 572, L1  
 Chapman S. C., Blain A. W., Ivison R. J., Smail I., 2003a, Nature, 422, 695  
 Chapman S. C., et al., 2003b, conference proceedings (astro-ph/0304236)  
 Cole S., Norberg P., Baugh C. M., et al., 2001, MNRAS, 326, 255  
 Conselice C.J., 2003, ApJS, 147, 1  
 Daddi E., Cimatti A., Pozzetti L., et al., 2000, A&A 361, 535  
 Daddi E., Cimatti A., Renzini A., 2000, A&A 362, L45  
 Daddi E., Broadhurst T. J., Zamorani G., et al., 2001, A&A, 376, 825  
 Daddi E., Cimatti A., Broadhurst T. J., et al., 2002, A&A 384, L1  
 Daddi E., Röttgering H., Labbé I., et al., 2003, ApJ, 588, 50  
 Dey A., Graham J. R., Ivison R. J., et al., 1999, ApJ, 519, 610  
 Franx M., Labbé I., Rudnick G., et al., 2003, ApJ, 587, L79  
 Genzel R., Baker A. J., Tacconi L. J., et al., 2003, ApJ, 584, 633  
 Giacconi R., Zirm A., Wang J., et al., 2002, ApJS, 139, 369  
 Giavalisco M., 2002, ARA&A, 40, 579  
 Giavalisco M., et al., 2003, this volume  
 Kellermann K.I., Fomalont E.B., Rosati P., Shaver P., 2003, in preparation  
 Kennicutt R. C., 1998, ARA&A, 36, 189  
 Labbé I., Rudnick G., Franx M., et al., 2003, ApJ, 591, L??  
 Labbé I., Franx M., Rudnick G., et al., 2003, AJ, 125, 1107  
 McCarthy P. J., Carlberg R. G., Chen H.-W., et al., 2001, ApJ, 560, L131  
 Meurer G. R., Heckman T. M., Calzetti D., 1999, ApJ, 521, 64  
 Nandra K., Mushotzky R. F., Arnaud K., et al., 2002, ApJ, 576, 625  
 Norberg P., Baugh C. M., Hawkins E., et al., 2002, MNRAS, 332, 827  
 Papovich C., Dickinson M., Ferguson H. C., 2001, ApJ, 559, 620  
 Pozzetti L., Cimatti A., Zamorani G., et al., 2002, A&A, 402, 837  
 Ranalli P., Comastri A., Setti G., 2003, A&A, 399, 39  
 Somerville R. S., Primack J. R., Faber S. M., 2001, MNRAS, 320, 504  
 Somerville R. S., Moustakas L. A., Mobasher B., et al., 2003, this volume  
 Shapley A., Steidel C.C., Pettini M., Adelberger K.L., 2003, ApJ, 588, 65  
 Smail I., Chapman S.C., Ivison R.J., et al., 2003 (astro-ph/0303128)  
 van Dokkum P. G., et al., 2003, ApJ, 587, L83  
 Webb T. M., Eales S. A., Lilly S. J., et al., 2003, ApJ, 587, 41